

RANDOMSEMO: NORMALITY LEARNING OF MOVING OBJECTS FOR VIDEO ANOMALY DETECTION

Chaewon Park*, Minhyeok Lee†, MyeongAh Cho‡ Sangyoun Lee§

School of Electrical and Electronic Engineering, Yonsei University, Seoul, Korea

ABSTRACT

Recent anomaly detection algorithms have shown powerful performance by adopting frame predicting autoencoders. However, these methods face two challenging circumstances. First, they are likely to be trained to be excessively powerful, generating even abnormal frames well, which leads to failure in detecting anomalies. Second, they are distracted by the large number of objects captured in both foreground and background. To solve these problems, we propose a novel superpixel-based video data transformation technique named Random Superpixel Erasing on Moving Objects (*RandomSEMO*) and Moving Object Loss (*MOLoss*), built on top of a simple lightweight autoencoder. *RandomSEMO* is applied to the moving object regions by randomly erasing their superpixels. It enforces the network to pay attention to the foreground objects and learn the normal features more effectively, rather than simply predicting the future frame. Moreover, *MOLoss* urges the model to focus on learning normal objects captured within *RandomSEMO* by amplifying the loss on the pixels near the moving objects. The experimental results show that our model outperforms state-of-the-arts on three benchmarks.

Index Terms— Video Anomaly Detection, Data Transformation, Frame Prediction, Superpixel, Moving Object

1. INTRODUCTION

Video anomaly detection (VAD) is a computer vision task that discriminates abnormal behaviors within the captured scenes. It is gaining interest due to the demanding cost on monitoring surveillance videos. Because the occurrence of abnormal events is rare compared to the normal, which is known as a data imbalance problem, the datasets used to develop anomaly detection models consist of a normal training set and a test set containing both normal and abnormal frames [1, 2, 3]. Following this circumstance, most of the deep-learning based VAD models [4, 5, 6, 7, 8, 9, 10] are trained to recognize the normal patterns during training, and detect the frames with the outlying patterns during testing. Some methods [4, 5, 6,

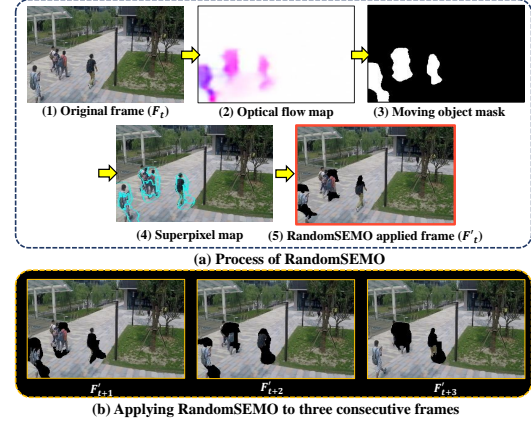


Fig. 1: Process of the proposed RandomSEMO. (a) shows the process done for each frame. With the optical flow computed between F_t and F_{t+1} ((2)), we estimate the region of the moving objects ((3)). Then, on that region, we group pixels with similar characteristics to make superpixels ((4)). Finally, we erase some superpixels at a random probability ((5)). (b) illustrates application on three successive frames.

9] utilize frame predicting autoencoders (AEs) which generate the successive frame from the input frames based on the learned normal patterns. These approaches discriminate abnormal scenes by the quality of the predicted output, assuming that the unusual frame is likely to be generated poorly.

However, these approaches face two major challenges. First, the AEs tend to perform excessively well, generating even the abnormal frames with high quality, which is adverse in detecting anomalies. Also, the large number of objects in the foreground and background distract the AE from focusing on the prominent moving objects. Abnormal behaviors generally take place in the moving foregrounds, rather than the background objects.

To cope with these problems, inspired by the recently proposed data transformation algorithms [9, 12, 13], we propose a novel video transformation technique named RandomSEMO. It is applied in the data pre-processing stage before feeding the input to the frame predicting AE during training phase. The RandomSEMO erases random superpixels found on the moving object regions. It works under the assumption that the model is likely to learn the most prominent objects'

*E-mail: chaewon28@yonsei.ac.kr

†E-mail: hydragon516@yonsei.ac.kr

‡E-mail: maycho0305@yonsei.ac.kr

§Corresponding Author, E-mail: sylee@yonsei.ac.kr

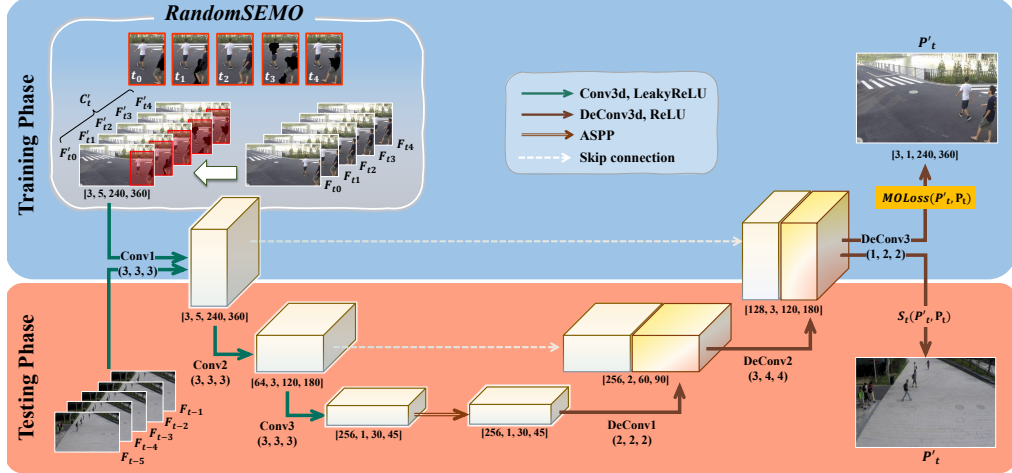


Fig. 2: Overall framework of our method. During training, the AE predicts future frame P'_t from the RandomSEMO input frames C'_t . The training exceeded with the help of the proposed MOLoss. When testing, the RandomSEMO is detached and normality score S_t obtained from the quality of P'_t determines the normality of each frame. The values in brackets indicate [channel, temporal, height, width] of feature and (depth, height, width) of kernel in order.

normal patterns when it is given partially insufficient data for the frame predicting task.

We also propose a Moving Object Loss (MOLoss) to maximize the effect of RandomSEMO. The MOLoss amplifies the loss of the pixels on the moving objects via generating a weight map. By utilizing the proposed loss function, our model is designed to focus on the foreground regions, effectively extracting crucial features with less distraction of the background objects.

Our contributions are summarized as: (1) We propose a superpixel-based video transformation method called RandomSEMO. (2) We maximize the advantage of the RandomSEMO with the proposed loss function, MOLoss. (3) Our model surpasses or performs compatibly with other methods.

2. RELATED WORKS

Various data transformation techniques, such as augmentations, have been proposed to boost the feature learning for computer vision tasks. In the image-level, Zhong *et al.* [14] introduced Random Erasing which makes occlusion at a random patch in the image. DeVries and Taylor [15] suggested CutOut, a method that deletes a box at the random location. These mentioned methods are all proven by experiments to enhance the performance of various tasks.

Few VAD methods have been proposed using the data transformation. Georgescu *et al.* [16] used sequence-reversed frames to embed motion feature learning. Park *et al.* [9] devised SRT and TMT, which rotates random rectangular patches in the spatial dimension and shuffles the sequence of random patches, respectively. Our work is in close relation with this method. However, compared to the work of Park *et al.* [9], our proposed RandomSEMO is fully aware of the moving objects and applied only on the corresponding region. It transforms the superpixels of the region, which

is more sophisticated and foreground-aware than applying transformations on random rectangular patches. Therefore, our method is more superior in the localizing ability, which is discussed in Sec. 4.2 and Fig. 5.

3. METHOD

The overall framework is described in Fig. 2. We resize N_f consecutive frames $F_{t-N_f}, F_{t-N_f+1}, F_{t-N_f+2}, \dots, F_{t-1}$ to $3 \times 240 \times 360$ and stack them to make a 4D cuboid $C_t \in \mathbb{R}^{3 \times N_f \times 240 \times 360}$. During training, RandomSEMO takes place to make transform C_t to C'_t . Then, C'_t is fed to the AE which generates a prediction of the future frame P'_t . The AE is trained with the proposed MOLoss between P'_t and the ground truth P_t . During inference, RandomSEMO is detached. C_t is fed to the AE, and the normality score S_t is calculated from P'_t to distinguish the abnormal frames.

3.1. RandomSEMO

We propose RandomSEMO, a transformation method that eliminates the details of the foregrounds by randomly erasing the superpixels of the moving objects. The purpose of RandomSEMO is to let AE be trained to extract prototypical normal features of the foreground objects than simply learning to predict frames well.

To apply RandomSEMO, we first localize the moving objects. Given a sequence of frames $F_{t-N_f}, F_{t-N_f+1}, F_{t-N_f+2}, \dots, F_{t-1}, P_t$, we compute the optical flow between each two successive frames (Fig. 1 (2)). Then, we generate moving object masks MoMask (Fig. 1 (3)) by thresholding the magnitude of the optical flow. Next, we apply SLIC [17] on the masked regions of the former frames to generate superpixel maps (Fig. 1 (4)) with maximum N_{sp} components. Finally, we randomly erase the superpixels by replacing the values with zero (Fig. 1 (5)). Each superpixel is erased with probability T_{sp} .

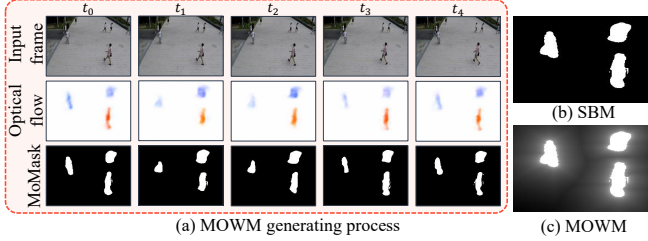


Fig. 3: MOWM generating process.

By utilizing RandomSEMO, the network is forced to learn the appearance and motion features of the moving objects to infer the future frame with the randomly erased information, as seen in Fig. 1 (b). This solves the aforementioned excessive predicting power problem of the previous methods because our method makes the model to focus on the normal feature learning, rather than simply implying the upcoming frame with the cues of the input frames. Also, the AE effectively extracts normal features because RandomSEMO nudges the model to pay attention to the moving objects which are more potentially abnormal than the background.

3.2. MOLoss

To maximize the effect of RandomSEMO, we optimize our model with the newly proposed MOLoss. MOLoss is a weighted sum of a moving object weighted L1 loss L_m and SSIM loss [18] L_s obtained between \mathbf{P}'_t and \mathbf{P}_t . L_m amplifies loss on the pixels near the moving objects by using a Moving Object Weight Map (MOWM). Fig. 3 shows the example and generating process of MOWM. We sum up all the MoMask obtained during RandomSEMO to generate a summed binary mask (SBM) (Fig. 3 (b)), which represents the moving object region of the input frame cuboid C'_t . Therefore, SBM is expressed as:

$$\text{SBM}_t = \min \left(\sum_{k=0}^{t-1} \text{MoMask}_k, 255 \right) \quad (1)$$

Then, we apply a distance function to SBM to generate MOWM, which demonstrates the inverse-distance from each pixel to the foreground. Thereby, the values near the foreground pixel are large and vice versa. MOWM is defined as:

$$\text{MOWM}^t = 255 - \begin{cases} \min \sqrt{(p_x - q_x)^2 + (p_y - q_y)^2} & , p \in \text{SBM}_{bg} \\ 0 & , p \in \text{SBM}_{fg} \end{cases} \quad (2)$$

where p and q indicate each pixel in SBM_t and its nearest foreground pixel, respectively. Evidently, the pixels near the foreground have relatively big values for the corresponding location in MOWM. Then, MOWM is multiplied during L1 loss calculation, amplifying the values near the moving objects. During this stage, we add a small value η to the tensorized MOWM to avoid zero values. Because L_m is a pixel-level loss function, we combine this with L_s to guarantee the similarity of \mathbf{P}'_t and \mathbf{P}_t in the feature-level. The equations are as follows:

$$L_m(\mathbf{P}'_t, \mathbf{P}_t) = \frac{1}{M \times N} \sum_{x=0}^{M-1} \sum_{y=0}^{N-1} [(\text{MOWM}^t_{(x,y)} + \eta) \times |\mathbf{P}'_{(x,y)} - \mathbf{P}_{(x,y)}|] \quad (3)$$

$$L_s(\mathbf{P}'_t, \mathbf{P}_t) = 1 - \frac{(2\mu_{\mathbf{P}'_t} \mu_{\mathbf{P}_t} + c_1)(2\sigma_{\mathbf{P}'_t \mathbf{P}_t} + c_2)}{(2\mu_{\mathbf{P}'_t}^2 \mu_{\mathbf{P}_t}^2 + c_1)(\sigma_{\mathbf{P}'_t}^2 + \sigma_{\mathbf{P}_t}^2 + c_2)} \quad (4)$$

In Eq. 3, M and N represent the number of pixels in the width and height axis, respectively. Moreover, x and y represent the location of each pixel in the width and height axis. In Eq. 4, μ and σ^2 denote the average and variance of each frame, respectively. Also, $\sigma_{\mathbf{P}'_t \mathbf{P}_t}$ represents the covariance. c_1 and c_2 are the variables to stabilize the division. Finally, MOLoss is described as:

$$\text{MOLoss}(\mathbf{P}'_t, \mathbf{P}_t) = w_m L_m(\mathbf{P}'_t, \mathbf{P}_t) + w_s L_s(\mathbf{P}'_t, \mathbf{P}_t) \quad (5)$$

where w_m and w_s denote the weights that control the contribution of L_m and L_s , respectively.

3.3. AE Architecture

The AE used in our method is trained to recognize the likelihood of the normal frames and predict the upcoming frame \mathbf{P}'_t from the transformed input frame cuboid C'_t using the learned normal features. To avoid excessive generalization, we design a lightweight, yet effective AE. As demonstrated in Fig. 2, our AE is composed of a three-layer encoder and a three-layer decoder with skip connections in between to supplement the features lost during downsampling. Each encoder layer consists of 3D convolution, batch normalization, and LeakyReLU activation. After the last encoder layer, an Atrous Spatial Pyramid Pooling (ASPP) [21] layer takes place to enlarge the receptive field. The decoder layers are all made of 3D deconvolution, batch normalization, and ReLU activation.

3.4. Normality Score

During inference, we adopt the peak signal to noise ratio (PSNR) to estimate the abnormality of each frame. It is defined as $\text{PSNR}(\mathbf{P}'_t, \mathbf{P}_t) = 10 \log_{10} \frac{\max(\mathbf{P}'_t)}{\|\mathbf{P}'_t - \mathbf{P}_t\|_2^2 / N}$, where N is the number of pixels in the frame. When \mathbf{P}_t contains anomalies which our network has never seen during training, our network is incapable of predicting a clear \mathbf{P}'_t , resulting in low PSNR and vice versa. Following [2, 11, 4, 7, 5, 10, 9, 8], we normalize $\text{PSNR}(\mathbf{P}'_t, \mathbf{P}_t)$ of each video clip to the range $[0, 1]$ to obtain the final normality score S_t .

$$S_t = \frac{\text{PSNR}(\mathbf{P}'_t, \mathbf{P}_t) - \min \text{PSNR}(\mathbf{P}'_t, \mathbf{P}_t)}{\max \text{PSNR}(\mathbf{P}'_t, \mathbf{P}_t) - \min \text{PSNR}(\mathbf{P}'_t, \mathbf{P}_t)} \quad (6)$$

4. EXPERIMENTS

Dataset. We validate our network on three popular benchmarks: CUHK Avenue [1], ShanghaiTech Campus (ST) [2], and UCSD Ped2 [3]. These datasets are all acquired by fixed cameras from the real-world. Among the three, ST [2] is the largest and most complex, containing 330 training videos and 107 testing videos captured from 13 different scenes.

Evaluation metric. For the evaluation, we adopt the area under curve (AUC) obtained from the frame-level scores and the ground truth labels. This metric is used in most studies [4, 7, 6, 9, 11, 12] on VAD. Since the first five frames of each clip cannot be predicted, they are ignored in the evaluation, following other prediction-based methods [4, 6, 5, 9].

Dataset \ Model	STAN [10]	Abn GAN [25]	HyAE [7]	Mem AE [11]	AD [26]	IntAE [6]	MNAD -Recon [5]	Fast Ano [9]	Base	Base+R	Base+R+M (Ours)
Avenue [1]	81.7	-	82.8	83.3	-	83.7	82.8	85.3	84.1	83.9	85.4
ST [2]	-	-	-	71.2	-	71.5	69.8	72.2	71.6	72.4	
Ped2 [3]	92.2	93.5	84.3	94.1	95.5	96.2	90.2	96.3	93.7	94.2	95.8
FPS	50	-	-	38	2	30	67	195	127	127	127

Table 1: Frame-level AUC (%) comparison. All figures and FPS are copied from the corresponding papers. 'Base' indicates our baseline framework without the RandomSEMO and MOLoss. It is instead trained with a single L_1 loss. R and M represent RandomSEMO and MOLoss, respectively. The top two results for each category are marked red and blue.

	Avenue [1]	Ped2 [3]
$T_{sp} = 0.1$	84.1	94.9
$T_{sp} = 0.2$	85.0	95.9
$T_{sp} = 0.3$	85.4	95.8
$T_{sp} = 0.4$	84.5	95.0
$T_{sp} = 0.5$	84.4	94.1
$T_{sp} = 0.6$	84.4	94.7

Table 2: Impact of the RandomSEMO probability T_{sp}

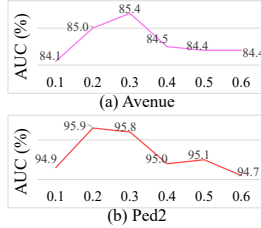


Fig. 4: Graph of Table 2

	Avenue [1]	ST [2]	Ped2 [3]
L_1	83.9	72.2	94.2
SSIM [18]	84.3	72.0	94.2
$w_m L_1 + w_s \text{SSIM}$ [18]	84.8	72.3	94.2
MOLoss	85.4	72.4	95.8

Table 3: Impact of MOLoss. Comparison with L_1 , SSIM [18], and a weighted sum of L_1 and SSIM [18].

Settings. We implement our experiments using PyTorch and a NVIDIA RTX A6000. Also, we use a pre-trained FlowNet2 [23] to generate optical flow maps. The training is based on batch size 30 and Adam optimizer with an initial learning rate of $2e^{-4}$, $\beta_1 = 0.5$, $\beta_2 = 0.9$. The network is trained for 40 epochs on Ped2 [3] and Avenue [1] and 10 epochs for ST [2]. η , w_m , w_s , N_f , N_{sp} , and T_{sp} are empirically set to 1, 0.25, 0.75, 5, 10, and 0.3 respectively.

4.1. Quantitative Results

The quantitative results are shown in Table 1. We compare our network with eight VAD networks that do not require any pre-trained network—such as object detectors or optical flow networks—during inference for fair comparison. It is observed that the accuracy of our model is superior to most of the compared methods in the three datasets. Furthermore, our proposed network is capable of detecting anomalies at 127 frames per seconds (FPS), faster than most methods. Because accuracy and speed are both mandatory in the real world application, our network is more practical than other methods that show low accuracy or slow speed.

4.2. Qualitative Results

Fig. 5 demonstrates the output and difference map of our network compared to those of FastAno [9]. The difference map shows that our network more precisely localizes the abnormal object. Only the biker is saturated in our proposed model whereas the background pixels near the biker is unnecessarily highlighted in FastAno [9], mirroring the effect of our moving object aware RandomSEMO and MOLoss. Furthermore,

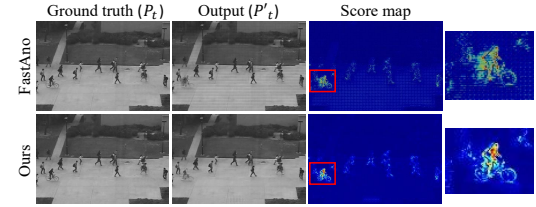


Fig. 5: Qualitative results on Ped2 [3] compared with those of FastAno [9]. The biker on the pedestrian street is the anomaly in this scene.

the difference between foreground and background is more pronounced in our results.

4.3. Impact of RandomSEMO probability T_{sp}

We found the optimal value of T_{sp} by changing T_{sp} from 0.1 to 0.6. Table 2 and Fig. 4 show the result of the experiments conducted on Avenue [1] and Ped2 [3]. For Avenue [1], the accuracy is highest when T_{sp} is 0.3. For Ped2 [3], the model trained with $T_{sp} = 0.2$ shows the best performance, and it is also as much accurate when trained with $T_{sp} = 0.3$. Furthermore, it is observed that both low T_{sp} leads to relatively low performance because only a few superpixels are obscured, practically having no significant difference from the original image. Similarly, the accuracy drops when T_{sp} is high because too much information is lost.

4.4. Impact of MOLoss

We conducted ablation studies to validate the contribution of MOLoss. The results are compared in Table 3. We experimented by changing the loss function to L_1 loss, SSIM loss, and a weighted sum of L_1 and SSIM where the weights are equivalent to those of the MOLoss. From the results, it is observed that using MOLoss strongly boosts the performance, especially when compared to using a single L_1 loss.

5. CONCLUSION

We propose a novel superpixel-based video transformation method called *RandomSEMO* for anomaly detection. Also, we propose a loss function named *MOLoss* to boost the effect of *RandomSEMO* by amplifying the loss values on the pixels near the moving objects. The experimental results have shown that our network performs competitively or surpasses other previous methods. Furthermore, we validated the impact of *RandomSEMO* and *MOLoss* with ablation studies and output comparison. As future works, we will verify the localizing ability of our model for extensive usage.

6. REFERENCES

- [1] Cewu Lu, Jianping Shi, and Jiaya Jia, “Abnormal event detection at 150 fps in matlab,” in *ICCV*, 2013, pp. 2720–2727.
- [2] Weixin Luo, Wen Liu, and Shenghua Gao, “A revisit of sparse coding based anomaly detection in stacked rnn framework,” in *ICCV*, 2017, pp. 341–349.
- [3] Vijay Mahadevan, Weixin Li, Viral Bhalodia, and Nuno Vasconcelos, “Anomaly detection in crowded scenes,” in *CVPR*. IEEE, 2010, pp. 1975–1981.
- [4] Wen Liu, Weixin Luo, Dongze Lian, and Shenghua Gao, “Future frame prediction for anomaly detection—a new baseline,” in *CVPR*, 2018, pp. 6536–6545.
- [5] Hyunjong Park, Jongyoun Noh, and Bumsub Ham, “Learning memory-guided normality for anomaly detection,” in *CVPR*, 2020, pp. 14372–14381.
- [6] Yao Tang, Lin Zhao, Shanshan Zhang, Chen Gong, Guangyu Li, and Jian Yang, “Integrating prediction and reconstruction for anomaly detection,” *PR Letters*, vol. 129, pp. 123–130, 2020.
- [7] Trong Nguyen Nguyen and Jean Meunier, “Hybrid deep network for anomaly detection,” *BMVC*, 2019.
- [8] MyeongAh Cho, Taeoh Kim, Ig-Jae Kim, and Sangyoun Lee, “Unsupervised video anomaly detection via normalizing flows with implicit latent features,” *arXiv preprint arXiv:2010.07524*, 2020.
- [9] Chaewon Park, MyeongAh Cho, Minhyeok Lee, and Sangyoun Lee, “Fastano: Fast anomaly detection via spatio-temporal patch transformation,” in *WACV*, 2022, pp. 2249–2259.
- [10] Sangmin Lee, Hak Gu Kim, and Yong Man Ro, “Stan: Spatio-temporal adversarial networks for abnormal event detection,” in *ICASSP*. IEEE, 2018, pp. 1323–1327.
- [11] Dong Gong, Lingqiao Liu, Vuong Le, Budhaditya Saha, Moussa Reda Mansour, Svetha Venkatesh, and Anton van den Hengel, “Memorizing normality to detect anomaly: Memory-augmented deep autoencoder for unsupervised anomaly detection,” in *ICCV*, 2019, pp. 1705–1714.
- [12] Muhammad Zaigham Zaheer, Jin-ha Lee, Marcella Astrid, and Seung-Ik Lee, “Old is gold: Redefining the adversarially learned one-class classifier training paradigm,” in *CVPR*, 2020, pp. 14183–14193.
- [13] Abhishek Joshi and Vinay P Namboodiri, “Unsupervised synthesis of anomalies in videos: transforming the normal,” in *IJCNN*. IEEE, 2019, pp. 1–8.
- [14] Zhun Zhong, Liang Zheng, Guoliang Kang, Shaozi Li, and Yi Yang, “Random erasing data augmentation,” in *AAAI*, 2020, vol. 34, pp. 13001–13008.
- [15] Terrance DeVries and Graham W Taylor, “Improved regularization of convolutional neural networks with cutout,” *arXiv preprint arXiv:1708.04552*, 2017.
- [16] Mariana-Iuliana Georgescu, Antonio Barbalau, Radu Tudor Ionescu, Fahad Shahbaz Khan, Marius Popescu, and Mubarak Shah, “Anomaly detection in video via self-supervised and multi-task learning,” in *CVPR*, 2021, pp. 12742–12752.
- [17] Radhakrishna Achanta, Appu Shaji, Kevin Smith, Aurelien Lucchi, Pascal Fua, and Sabine Süsstrunk, “Slic superpixels,” *Tech. Rep.*, 2010.
- [18] Hang Zhao, Orazio Gallo, Iuri Frosio, and Jan Kautz, “Loss functions for image restoration with neural networks,” *IEEE Transactions on computational imaging*, vol. 3, no. 1, pp. 47–57, 2016.
- [19] Du Tran, Lubomir Bourdev, Rob Fergus, Lorenzo Torresani, and Manohar Paluri, “Learning spatiotemporal features with 3d convolutional networks,” in *ICCV*, 2015, pp. 4489–4497.
- [20] Andrew L Maas, Awni Y Hannun, Andrew Y Ng, et al., “Rectifier nonlinearities improve neural network acoustic models,” in *ICML*. Citeseer, 2013, vol. 30, p. 3.
- [21] Liang-Chieh Chen, George Papandreou, Iasonas Kokkinos, Kevin Murphy, and Alan L Yuille, “Deeplab: Semantic image segmentation with deep convolutional nets, atrous convolution, and fully connected crfs,” *TPAMI*, vol. 40, no. 4, pp. 834–848, 2017.
- [22] Vinod Nair and Geoffrey E Hinton, “Rectified linear units improve restricted boltzmann machines,” in *ICML*, 2010.
- [23] Eddy Ilg, Nikolaus Mayer, Tonmoy Saikia, Margret Keuper, Alexey Dosovitskiy, and Thomas Brox, “Flownet 2.0: Evolution of optical flow estimation with deep networks,” in *CVPR*, 2017, pp. 2462–2470.
- [24] Diederik P Kingma and Jimmy Ba, “Adam: A method for stochastic optimization,” *arXiv preprint arXiv:1412.6980*, 2014.
- [25] Mahdyar Ravanbakhsh, Moin Nabi, Enver Sangineto, Lucio Marcenaro, Carlo Regazzoni, and Nicu Sebe, “Abnormal event detection in videos using generative adversarial nets,” in *ICIP*. IEEE, 2017, pp. 1577–1581.
- [26] Mahdyar Ravanbakhsh, Enver Sangineto, Moin Nabi, and Nicu Sebe, “Training adversarial discriminators for cross-channel abnormal event detection in crowds,” in *WACV*. IEEE, 2019, pp. 1896–1904.
- [27] Fei Dong, Yu Zhang, and Xiushan Nie, “Dual discriminator generative adversarial network for video anomaly detection,” *IEEE Access*, vol. 8, pp. 88170–88176, 2020.